Hydrol. Earth Syst. Sci. Discuss., doi:10.5194/hess-2016-208, 2016
Manuscript under review for journal Hydrol. Earth Syst. Sci.
Published: 9 May 2016

Hydrology and Earth System Sciences
Open Access
EGU
Discussions

Seasonal Dynamics of Rainfall Erosivity in Switzerland

Simon Schmidt[1], Christine Alewell[1], Panos Panagos[2], Katrin Meusburger[1]

[1]Environmental Geosciences, University Basel, Bernoullistrasse 30, CH-4056 Basel, Switzerland
[2]European Commission, Joint Research Centre, Institute for Environment and Sustainability, Via E. Fermi 2749, I-21027 Ispra, Italy

Correspondence to: Simon Schmidt (si.schmidt@unibas.ch)

Abstract. One major controlling factor of water erosion is rainfall erosivity, which is quantified by the kinetic energy of a rainfall event and its maximum 30-min intensity. Rainfall erosivity is often expressed as R-factor in soil erosion risk models like the Universal Soil Loss Equation (USLE) and its revised version (RUSLE). As rainfall erosivity is closely correlated with dynamic rainfall amount and intensity, the rainfall erosivity of Switzerland can be expected to have a characteristic regional and seasonal dynamic throughout the year. This intra-annual variability was mapped by a monthly modelling approach to assess simultaneously spatial and monthly pattern of rainfall erosivity. So far only national seasonal means and regional annual means exist for Switzerland. We used a network of 87 precipitation gauging stations with a 10-minute temporal resolution to calculate long-term monthly mean R-factors. Stepwise regression and Leave-one-out cross-validation (LOOCV) were used to select spatial covariates which explain the spatial and temporal pattern of the R-factor for each month across Switzerland. The monthly R-factor is mapped by its specific regression equation and the ordinary kriging interpolation of its residuals (Regression-Kriging). As covariates, a variety of precipitation indicator data has been included like snow depths, a combination product of hourly precipitation measurements and radar observations (CombiPrecip), daily alpine precipitation (EURO4M-APGD) and monthly precipitation sums (RhiresM). Topographic parameters (elevation, slope) were also significant explanatory variables for single months. The comparison of the 12 monthly rainfall erosivity maps showed a distinct seasonality with highest rainfall erosivity in summer (June, July, and August) influenced by intense rainfall events. Winter months have lowest rainfall erosivity. A proportion of 62% of the total annual rainfall erosivity is identified within four months only (June to September). Highest erosion risk can be expected for July where not only rainfall erosivity but also erosivity density is high. Additionally to the intra-annual temporal regime, a spatial variability of this seasonality was detectable between different regions of Switzerland. The assessment of the dynamic behavior of the R-factor is valuable for the identification of susceptible seasons and regions.

Keywords: R-factor, RUSLE, erosivity density, cumulative daily R-factor, erosion modelling, dynamic soil erosion risk assessment, seasonality, monthly erosivity

Hydrol. Earth Syst. Sci. Discuss., doi:10.5194/hess-2016-208, 2016
Manuscript under review for journal Hydrol. Earth Syst. Sci.
Published: 9 May 2016

Hydrology and Earth System Sciences
Open Access
Discussions

1 Introduction

Soil erosion by water is a major environmental issue in Switzerland which has been measured (Konz et al., 2012, Alewell et al., 2014), mapped (Mosiman, 1990; Prasuhn, 2011; Prasuhn, 2012), and modelled (Gisler et al., 2011; Prasuhn et al., 2013) extensively. Since the 1950s, soil erosion by water is increasing in Switzerland on ~~land under~~ arable land (Weisshaidinger & Leser, 2006) as well as in mountain grasslands (Meusburger & Alewell, 2008). Mosimann et al. (1991) assessed a quantity of up to 20% of all cultivated land in Switzerland to be affected by soil erosion. The costs of soil erosion for Switzerland's arable land were estimated to be about 53 million CHF yr-1 (US $55.2 million yr-1; Ledermann, 2012). Increasing trends of water erosion are predicted for Switzerland under future climate change due to more frequent and heavy precipitation during winter month (Fuhrer et al., 2006). Trends towards increasing rainfall erosivity are already observable in the months May to October (Meusburger et al., 2012).

Rainfall has direct impacts on soil mobilization by processes like rapid wetting or splash and runoff effects and is, therefore, one of the main driving forces of water erosion. The R-factor~~, one of the five soil erosion risk factors (rainfall erosivity, soil erodibility, slope steepness and length, cover management, and support practices)~~ of the Revised Universal Soil Loss Equation (RUSLE) (Renard et al., 1997; Foster et al., 2008) expresses the impact of rainfall on soils as rainfall erosivity. ~~The RUSLE is widely used for calculating soil loss, but each of the five factor maps also has an essential message on its own.~~ Besides being an important driving factor of soil erosion, the R- factor can also be used to conclude on soil vulnerability, flood hazard, and natural hazards or probability of droughts (Panagos et al.; 2015a).

Previously published studies on rainfall erosivity in Switzerland focused on national seasonal means (Panagos et al., 2015a) or regional annual means (Friedli, 2006; Gisler et al., 2011; Meusburger et al. 2012; Prasuhn et al., 2013;). Since Switzerland has ~~large regional and altitudinal variety in climatic conditions~~ (humid continental to oceanic climate; Köppen, 1936), seasonal and temporal variations of the weather are consequential. As such, these spatio-temporal variations can be expected to influence patterns in the rainfall erosivity. Meusburger et al. (2012) already showed the presence of a strong seasonality of the rainfall erosivity for clustered stations at different ~~altitudinal~~ classes in Switzerland. However, simultaneously spatial and temporal pattern of the R-factors ~~seasonality~~ have not yet been established. These spatio-temporal patterns are decisive in combination with spatio-temporal patterns of vegetation cover in order to allow for an accurate soil erosion risk assessment and relevant for a monthly and seasonal management of agriculture practices and hazard controls.

Here, we aim to assess the spatio-temporal ~~seasonal~~ variability of rainfall erosivity in Switzerland by

(i) extending the network of gauging stations from Meusburger et al. (2012) to obtain rainfall erosivity events for Switzerland

(ii) producing monthly R-factor maps based on high resolution spatial covariates using a regression-kriging approach

(iii) evaluate the spatio-temporal patterns of the ~~seasonal~~ R-factor dynamic in Switzerland

Hydrol. Earth Syst. Sci. Discuss., doi:10.5194/hess-2016-208, 2016
Manuscript under review for journal Hydrol. Earth Syst. Sci.
Published: 9 May 2016

Hydrology and Earth System Sciences
Discussions

2 Material and Methods

2.1 Rainfall erosivity (R-factor) calculation

The rainfall erosivity expressed as R-factor in RUSLE is a product of the kinetic rainfall energy (er) of an erosive rainfall event and its corresponding maximum intensity over a time span of 30 minutes (I30) (Brown & Forster, 1987). We used the erosive rainfall event thresholds defined by Renard et al. (1997) which were modified by Meusburger et al. (2012). The unit rainfall energy (er) (MJ ha-1 mm-1) for each time interval is expressed as the intensity of rainfall (ir) (mm h-1) during that time interval. It is calculated by Brown and Forster (1987) as:

$$e_r = 0.29[1 - 0.72\exp(-0.05i_r)] \quad (1)$$

The erosive rainfall event erosivity (EI30) (MJ mm ha-1¬ h-1¬) is a product of the unit rainfall energy (er) (Eq. (1)) and its maximum rainfall amount within a 30 minutes interval (according to Wischmeier & Smith, 1978):

$$EI_{30} = (\sum_{r=1}^{k} e_r v_r) I_{30} \quad (2)$$

where vr is the rainfall volume (mm) during a time unit r and I30 is the maximum rainfall intensity within 30 minutes of the event (mm h-1).

The monthly rainfall erosivity (R) (MJ mm ha-1¬ h-1¬ month-1) is the mean of the accumulated event erosivity (EI30) (Eq. (2) within a month:

$$R = \frac{1}{n}\sum_{j=1}^{n}\sum_{k=1}^{m_j}(EI_{30})_k \quad (3)$$

where n is the recorded number of years with the number of erosive events (mj) within a certain month j. k is the index of a single event with its corresponding event erosivity.

The event rainfall erosivity was calculated from the 10-min precipitation data for each station by applying the algorithm of Meusburger et al. (2012). The event rainfall erosivity was averaged by months to a long-term monthly mean R-factor (Rmo). Usually, snow, snowmelt and rainfall on frozen soil are not assessed in the R-factor (Renard et al.; 1997). Thus, a temperature threshold of 0°C was set to obtain only rainfall and exclude snow water equivalents which are subject to uncertainty in rainfall erosivity assessments (Leek & Olsen, 2000). Temperature data was measured simultaneous to precipitation (for 71 stations) or was directly derived (for 15 stations) from the closest stations (within a distance of less than 20 km) with similar elevation. We assumed only minor variation in temperature within that distance at a similar elevation level.

Besides neglecting snow, we did not consider rainfall as hail which is mainly occurring during summer in Switzerland (Nisi et al., 2016; Punge & Kunz, 2016). Hurni (1978) investigated the impact of hail on rainfall erosivity in Switzerland and concluded that the erosivity of hail exceeds the one of rainfall.

2.2 Stations

We extended the gauging station network of Meusburger et al. (2012) (10 minutes measuring intervals) from 71 to an updated dataset of 87 stations (Fig. 1).

Hydrol. Earth Syst. Sci. Discuss., doi:10.5194/hess-2016-208, 2016
Manuscript under review for journal Hydrol. Earth Syst. Sci.
Published: 9 May 2016

Hydrology and Earth System Sciences
Open Access
Discussions

The additional 16 stations were previously investigated for rainfall erosivity by Nogler (2012). On average, the network represents one station each ~~22 km x 22 km~~. The average distance of one station to all others is 113.6 km by a minimum distance to the closest station of 13.2 km. A majority of stations (63) have recorded data of at least 22~~yr~~. The mean length of observations is 19.5yr and thus, meet the proposed minimum time-scale requirements for rainfall erosivity calculations of a 15yr measuring period (Forster et al. 2008). The stations are well distributed and were subject to a quality control (Begert et al., 2005; Nogler, 2012).

2.3 Data and Covariates

High temporal information on snow cover and snow water equivalents, high spatio-temporal information on rainfall and high spatial information on topography are acquired as covariates (Table 1) for the monthly erosivity maps since rainfall erosivity is mainly controlled by precipitation and relief parameters (Meusburger et al., 2012; Panagos et al., 2015a; Panagos et al., 2016b). All data have a much higher resolution than datasets used in previously R-factor studies for Europe (Panagos et al., 2015a; 2016a) and Switzerland (Meusburger et al., 2012).

The long-term snow depth (derived from total snow depth monthly mean by MeteoSwiss) on a monthly resolution was used as an approximation for precipitation as snow. The monthly point data of snow depth was regionalized by Inverse Distance Weighting. Hourly Swiss CombiPrecip data (geostatistical combination of rain gauge measurements (150 automatic stations) and three C-band radar observations; Sideris et al., 2014) was aggregated and averaged to a long-term monthly mean. Long-term mean daily precipitation per month was calculated based on the daily values of alpine precipitation in EURO4M-APGD (Isotta et al., 2014). Averaging the monthly spatial precipitation of RhiresM (MeteoSwiss, 2013) over the years leads to long-term monthly mean precipitation sums. The variables elevation, slope, and aspect are retrieved from a Digital Terrain Modell (SwissAlti3D) for Switzerland.

2.4 Mapping the seasonal variability of rainfall erosivity in Switzerland

We used regression-kriging (Hengl et al., 2004; Hengl, 2007; Hengl et al., 2007) to map the monthly variability of rainfall erosivity. The regression-kriging approach relies on the monthly mean rainfall erosivities for each of the 87 stations which are going to be explained by a generalized linear regression (GLM). Later, the GLM is used for interpolating R_{mo} for Switzerland based on the spatial covariates. In an ordinary global kriging, the residuals of the regression are interpolated. The combination of R_{mo} with its residuals also enables the consideration of the standard error. Meusburger et al. (2012) discussed different interpolation methods for an annual mapping of rainfall erosivity in Switzerland. Their results show that regression-kriging is an adequate method for Switzerland if significant relations between rainfall erosivity and spatial covariates exist.

Leave-one-out cross-validation (LOOCV) (Efron & Tibishirani, 1997) was used to avoid a resampling-bias of the 87 R_{mo} for each month in the regression. Data-split is only valid for large n, otherwise it reduces the training observations, is random and limited in reproducibility (Steyerberg, 2009; Harrell, 2015). In consideration of the low number of n (n=87), LOOCV

Hydrol. Earth Syst. Sci. Discuss., doi:10.5194/hess-2016-208, 2016
Manuscript under review for journal Hydrol. Earth Syst. Sci.
Published: 9 May 2016

omits only one observation from the dataset per run and estimates the model from the remaining n-1 observations. The process was repeated 100 times for a better accuracy.

A log-transformation of R_{mo} resulted in a normal distribution of the data. The suitability of each covariate for the GLM was determined by an automated stepwise feature selection process according to the Akaike information criterion (AIC). The significance threshold for covariate selection was set to 0.1. We also tested Least Absolute Shrinkage and Selection Operator (LASSO) as an alternative feature selection method to the stepwise GLM, but it was less transparent for evaluation and showed inappropriate residual diagnostics (systematic error). Both, the LOOCV stepwise regression, as well as LASSO, were performed in the R-package "caret" (v6.0-68). Outliers (Bonferroni-adjusted outlier test) and influential observations (Cook's Distance) were omitted in the stepwise GLM.

The goodness-of-fit of the model was described by the coefficient of determination (R^2), the root mean square error (E_{RMS}) and the deviance. Regression diagnostics to evaluate the model included normality, non-constant error variance (homoscedasticity), multicollinearity (variance inflation factor; vif) and autocorrelation.

Twelve monthly maps of the long-term mean R_{mo} were derived by applying the regression equation with the covariates and their corresponding coefficients according to the individual monthly regression equation. The residuals of each month stepwise GLM were interpolated by an ordinary global kriging with a stable variogram model and added to the R_{mo} maps in ESRI ArcGIS (v.10.2.2.) afterwards.

Each monthly map is subject to an individual GLM. Therefore, a subset of individual covariates explains rainfall erosivity for each month separately. A combination of three monthly maps leads to long-term seasonal mean R-factor (R_{seas}) maps for Switzerland with high spatial resolution. In addition, the sum of all twelve maps results in an updated (compared to Meusburger et al., 2012) long-term annual mean R-factor (R_{year}) map. Improvements of the new map are the extended network of gauging stations, the cross-validation of the regression-kriging approach, and the inclusion of new high spatio-temporal covariates in order to increase the spatial resolution of the maps.

2.5 Cumulative daily R-factors

The cumulative percentage of R-factor is obtained and grouped by Swiss biogeographic regions to obtain the share of the total annual rainfall erosivity for Switzerland by seasons. These regions show distinct differences in climate, soils, elevation, steepness, and geographic location. The cumulative curve of rainfall erosivity events enables the extraction of the annual share of rainfall erosivity on a daily scale. Therefore, all recorded rainfall events measured at stations within an individual biogeographic unit are averaged on a daily level.

2.6 Monthly erosivity density

Monthly erosivity density (ED_{mo}) (MJ ha^{-1} h^{-1}) is calculated by the long-term ratio of R_{mo} (MJ mm ha^{-1} h^{-1} $month^{-1}$) to mean monthly precipitation amount (P_{mo}) (mm ~~month^{-1}~~) (Foster et al., 2008):

Hydrol. Earth Syst. Sci. Discuss., doi:10.5194/hess-2016-208, 2016
Manuscript under review for journal Hydrol. Earth Syst. Sci.
Published: 9 May 2016

Hydrology and Earth System Sciences Discussions

$$ED_{mo} = \frac{R_{mo}}{P_{mo}} \quad (4)$$

Smaller values of ED_{mo} indicate that the influence of monthly precipitation on the monthly rainfall erosivity is mainly driven by its amount. On the other hand, high values of ED_{mo} show that relative to the absolute rainfall amount a high kinetic energy of rainfall was observed (e.g., strong storm events; Panagos et al., 2016b). Highest soil erosion risk is expected for areas where rainfall erosivity is high but related to a few intense rainfall events (small P_{mo}) instead of a high monthly precipitation amount. As such, ED_{mo} can reflect the temporal variability of rainfall intensity (Dabny et al., 2011) and can indicate how precipitation (short duration events with high intensities or high amounts of rainfall) controls the seasonality of rainfall. For the calculation of ED_{mo}, we used RhiresM as the monthly precipitation dataset. According to Dabny et al. (2012), erosivity density is relatively independent of elevation up to a height of 3000 m a.s.l.. Only the station Piz Corvatsch exceeds that threshold of height (Dabny et al., 2012).

3 Results and Discussion

3.1 Monthly rainfall erosivity at the 87 Swiss gauging stations

R_{mo} data averaged for all investigated stations show a bell-shaped curve over the twelve months (Fig. 2) with an increasing trend starting from February (17.3 MJ mm ha^{-1} h^{-1} month^{-1}) to a maximum in July (289 MJ mm ha^{-1} h^{-1} month^{-1}). The mean R_{mo} per months is 112 MJ mm ha^{-1} h^{-1} ~~month^{-1}~~. The meteorological season winter (Dec-Jan-Feb) has the lowest mean Rmo (33 MJ mm ha^{-1} h^{-1} month^{-1}), followed by spring (Mar-Apr-May) (68 MJ mm ha^{-1} h^{-1} ~~month^{-1}~~), fall (Sep-Oct-Nov) (92 MJ mm ha^{-1} h^{-1} ~~month^{-1}~~) and summer (Jun-Jul-Aug) (257 MJ mm ha^{-1} h^{-1} ~~month^{-1}~~).

Most of the monthly R-factors (96%) of the lowest 10% of all monthly values are part of the period between November and April whereas 97% of the highest 10% are monthly rainfall erosivities from May to October.

The recently published "Monthly Rainfall Erosivity" for Europe by Panagos et al. (2016a) and the national observations of Mosimann et al. (1990) for a single station in Switzerland (Bern, Swiss Midland) fit the present calculations with highest rainfall erosivity for the season from June/July to August. The Swiss monthly rainfall erosivities in the European assessment (Panagos et al., 2016a) are smaller on average by 3 MJ mm ha^{-1} h^{-1} ~~month^{-1}~~ (after rescaling with the calibration factors from 30 to 10 minutes). That discrepancy by 5% mainly arises due to the different numbers and time series of gauging stations (87 vs. 71).

Seasonality of R_{mo} is also observed for Italy (Borrelli et al., 2016), Greece (Panagos et al., 2016b), Iran (Sadeghi et al., 2011), Chile (Bonilla & Vidal, 2011), El Salvador (da Silva et al., 2010) and regions of Australia (Yang & Yu, 2015), China (Zhao et al., 2015), Korea (Arnhold et al., 2014), the Himalayas (Xing et al., 2014), and Brazil (da Silva et al., 2013). However, the timing of the maximum and minimum erosivity varies considerably. Some of the other studies show highest values in fall and winter (Greece), highest values in March and lowest values in July (Iran), or highest values in January and lowest values in July (Australia). The seasonal R_{mo} in Italy and Greece have lower ranges (209 and 121 MJ mm ha^{-1} h^{-1}

Hydrol. Earth Syst. Sci. Discuss., doi:10.5194/hess-2016-208, 2016
Manuscript under review for journal Hydrol. Earth Syst. Sci.
Published: 9 May 2016

Hydrology and Earth System Sciences Discussions

month^{-1}, respectively, compared to 272 MJ mm ha^{-1} h^{-1} month^{-1} in Switzerland), and the peak of the R-factor is shifted from July to September for Italy and November for Greece respectively.

3.2 Mapping of monthly rainfall erosivity and related uncertainties

All covariates – aspect excluded – were significant (p-value < 0.1) within the stepwise regressions for at least one month to explain R_{mo} (Table 2). For each month, an individual selection of covariates was achieved by the stepwise GLM.

Model efficiency averaged over all twelve months has a mean R^2 of 0.51 and a mean E_{RMS} of 0.61 MJ mm ha^{-1} h^{-1} month^{-1}. R^2 varies between 0.10 (Nov) and 0.66 (July). E_{RMS}s ranges from 0.93 to 0.42 MJ mm ha^{-1} h^{-1} month^{-1}. Regression functions for November and December are the most uncertain ones with lowest R^2 and highest E_{RMS} which need to be improved by additional covariates in the future, explaining rainfall erosivity in winter better. The low R^2s are arising due to the lower rainfall erosivity mainly caused by the higher amount of snow (neglected in this study), which makes it more challenging obtain better results. The same constrain was observed in a study for Greece with lowest rainfall erosivities and at the same time lowest R^2 (Panagos et al., 2016b). The higher the ratio of the null deviance to the residual deviance, the better the model fits by including the covariates. The residual deviance is lower than the null deviance in all twelve investigated months. Monthly model efficiency and omitted influential outliers to increase the model's goodness of fit are summarized in Table 3.

The monthly observations of R_{mo} at the 87 locations (exclusive outliers) as well as the residuals are normally distributed after the log-transformation. A non-constant error (homoscedasticity), multicollinearity and non-autocorrelation were determined for all observations of the twelve months. H_0 was rejected by the Breusch-Pagan-test in all cases to confirm homoscedasticity. Regression diagnostics further show a vif<4 for each month. Therefore, we could not identify collinear data. According to a Durbin-Watson-test, the Swiss R_{mo}-dataset is not autocorrelated.

The kriging of the residuals based on a stable variogram improved the interpolation in all months. The ranges of the variograms exceed the mean distance (approx. 13.2 km) of neighboring stations in all months. The average prediction error of all 12 months is -0.0055 by an averaged root mean square standard error of 1.046 MJ mm ha^{-1} h^{-1} month^{-1}. The used stable semivariogram models are represented by 12 lag classes. The standard deviation maps of the monthly residual kriging show the usual pattern with lowest standard deviations close to the stations and higher standard deviations with increasing distance from the gauging stations.

3.3 Monthly rainfall erosivity maps for Switzerland

~~Temporal patterns~~ of modelled R_{mo} show a distinct seasonality with national means being lowest in January (10.5 MJ mm ha^{-1} h^{-1} ~~month^{-1}~~) and highest in August (263.5 MJ mm ha^{-1} h^{-1} ~~month^{-1}~~) (Table 4, Fig. 3).

Winter is the season with the lowest rainfall erosivity. The highest R_{mo} peak in summer is consistent with the map of extreme point rainfall of 1h duration (100-year return period; Spreafico & Weingartner, 2005), where the strong influence of extreme rainfall events on rainfall erosivity is indicated. Meusburger et al. (2012) already pointed to the relationship of thunderstorm activity to annual rainfall erosivity. The thunderstorm season in Switzerland lasts from late spring (May) to early fall

Hydrol. Earth Syst. Sci. Discuss., doi:10.5194/hess-2016-208, 2016
Manuscript under review for journal Hydrol. Earth Syst. Sci.
Published: 9 May 2016

Hydrology and Earth System Sciences
Discussions

(September). Thunderstorms ~~cause high amounts of rainfall within a short time-period (intense rainfall) and, therefore,~~ are at least partly responsible for the high values of rainfall erosivity in summer. Starting from early fall (September), a decreasing trend of R_{mo} is noticeable all over Switzerland.

Averaged months are aggregated to representative seasons (R_{seas}) to identify spatial differences (Fig. 4).

Mean winter rainfall erosivity shows highest values in the Jura Mountains, western and eastern parts of the Northern Alps and the Southern Alps (canton Ticino). High winter rainfall erosivity can be explained by rainfall resulting from low-pressure areas in Northern Europe and weather fronts moved by north-westerly winds. These fronts are uplifted at the Jura Mountains what results in orographic rainfall. In spring, the Northern and the Southern Alps become more affected by high rainfall erosivity. The spatial variability of rainfall erosivity in spring in the Southern Alps (canton Ticino) corresponds to the air flow from the south and the onset of the thunderstorm season in that region which causes intense rainfall. High rainfall erosivities are persisting from spring to fall in the Southern Alps. High summer R-factors in the Southern Alps, the Jura Mountains and the Northern alpine foothill are influenced by thunderstorms which have their main impacts in these regions (van Delden, 2001; Perroud & Barder, 2013; Nisi et al., 2016; Punge & Kunz, 2016). Furthermore, the high rainfall erosivity in summer in the Southern Alps can be explained by high intense rainfall originating from orographic uplifts (Schwarb et al. 2011; Perroud & Barder, 2013). The cantons of Valais and Grisons remain with relatively low rainfall erosivity among all seasons. This is due to lower convection and thereby lower rainfall erosivity in summer.

The map showing the range (Fig. 5) indicates the degree of maximal variation at a certain location along a year and is the difference between ~~minamum~~ and maximum monthly rainfall erosivity of all 12 months. The highest range (up to 6086 MJ mm ha^{-1} h^{-1} ~~month^{-1}~~) is apparent in the canton Ticino at the Southern Alps. Also the Northern Alps, Swiss Midland and Jura Mountains show a high variation within a year. The Eastern and Western Central Alps have lowest ranges in accordance with their relatively low rainfall erosivity among the year.

Compared to the rainfall erosivity evaluation by Meusburger et al. (2012) on an annual scale, the range of the observed mean R_{year} and spatial pattern did only change slightly due to the extended station network and high resolution spatial covariates (aggregated by all twelve monthly R-factor-maps).

3.4 Cumulative daily rainfall erosivity

Generally, steepest slopes of the cumulative rainfall erosivity curve for Switzerland is from June to September with a share of 62% of the total annual rainfall erosivity within these 4 months (Fig. 6). This proportion exceeds the average share of Europe of 53% during the same period (Panagos et al., 2016a). A much larger proportion (90%) of cumulative percentage of daily rainfall erosivity was observed by Schwertmann et al. (1987) for Bavaria. Mosimann et al. (1990) showed in a single-station approach (Bern, Swiss Midland) that a proportion of 80% of the total annual erosivity occurs in the period from April to September, which complies with the mean of 77% during the same period of a year resulting from the presented multi-station (87) calculation.

Hydrol. Earth Syst. Sci. Discuss., doi:10.5194/hess-2016-208, 2016
Manuscript under review for journal Hydrol. Earth Syst. Sci.
Published: 9 May 2016

Hydrology and Earth System Sciences Discussions

All biogeographic units in Switzerland have similar trends of the cumulative daily rainfall erosivity. Highest proportions (from Jun to Sep) and, therefore, steepest slopes can be identified for the Southern Alps with a share of 70% of the total sum. This high percentage of rainfall erosivity within a short period of time (4 months) is likely to have a large impact on the soil erosion susceptibility since it may coincide with lowest (after harvesting of crops, carrots, etc.) and unstable vegetation cover (after late sowing) (Hartwig & Ammon, 2002; Wellinger et al., 2006; Torriani et al., 2007; Prasuhn 2011). Furthermore, fully grown pre-harvest field crops (e.g. cereals, maize) might suffer by bend-over of corn stalks due to high intensity storms. In addition, water saturated conditions which are usual in May and September/October makes soils even more erodible. Highly susceptible soils may also be expected in areas cleared by forest fires in summer (which is the case especially for Ticino) (Marxer, 2003). The combination of the monthly rainfall erosivity maps with dynamic monthly C-factors might enable a monthly soil erosion risk assessment for Switzerland.

3.5 Seasonal erosivity density

Erosivity density (expressed as monthly ratios of R_{mo} to P_{mo}) can be used to distinguish between high rainfall erosivity which is mainly influenced by high rainfall amounts and those which is influenced by relatively low rainfall amounts but highly intense rainfalls. That distinction helps to evaluate the potential consequences of rainfall erosivity for each month. The ~~combination of high rainfall erosivity and low precipitation amounts (~~high erosivity density value~~)~~ is severe for soils since extreme rainfalls might meet dry and thus unstable soil and vegetation systems. The maps (Fig. 7) show that the influence of rainfall intensity on rainfall erosivity also underlies seasonal and spatial variations.

ED_{mo} in winter is lower than 1 MJ ha^{-1} h^{-1} (Fig. 7) for Switzerland. Therefore, rainfall intensity is not the driving factor for rainfall erosivity in these months where low rainfall erosivity meets high rainfall amounts. The relative high R_{mo} in the Jura Mountains is therefore mainly driven by large amounts of rainfall instead of high ~~intensified~~ rains.

ED_{mo} has a maximum for Switzerland in July (1.8 MJ ha^{-1} h^{-1}) which results from a relatively low rainfall amount indicating that rainfall erosivity is mainly controlled by high intensify events. Intense summer rainfall has its maximum in the regions of Jura, Swiss Midland, northern Alpine foothill, and Ticino. In these regions, R_{mo} is high accompanied by relative low precipitation amounts. As such, the erosivity risk is the highest within the year especially when soils are dry during periods of rare but high rainfall intensities and therefore, infiltration is reduced due to crusts.

The distribution of the Swiss ED_{mo} (Fig. 8) marks a bell-shaped curve as it also the case for investigated stations in the United States, Italy and Austria (Forster, 2008; Dabny et al., 2012; Borrelli et al., 2016; Panagos et al., 2016a). The monthly erosivity density of the neighboring country Austria complies with the Swiss values only with minor variability. Greece, Italy and the stations of the US are characterized by higher ED_{mo} values than Switzerland. Nonetheless, the conclusion Panagos et al. (2016b) drew for Greece ~~(Panagos et al., 2016b)~~ that "rainfall erosivity is not solely dependent on the amount of precipitation" is also generally valid for Switzerland.

Hydrol. Earth Syst. Sci. Discuss., doi:10.5194/hess-2016-208, 2016
Manuscript under review for journal Hydrol. Earth Syst. Sci.
Published: 9 May 2016

Hydrology and Earth System Sciences
Open Access
Discussions

4 Conclusion and Outlook

The main goal of the current study was to investigate the seasonal and regional variability of rainfall erosivity in Switzerland. A crucial advancement of the present research was to identify spatial and temporal windows of high erosivities. Through the spatial-temporal mapping, it was possible to identify regions that are hardly affected by rainfall erosivity ~~such as Grisons and Wallis~~ and it was also possible to identify regions that are affected in a certain month, such as Jura Mountains. The spatio-temporal variability of rainfall erosivity of Switzerland enables the controlled and time-dependent management of agriculture (like selective erosion measures, crop selection, time-dependent sowing) and droughts, ecosystem services evaluation, as well as the use for seasonal and regional hazard prediction (e.g. flood risk control, landslide susceptibility mapping). Rainfall erosivity based on high erosivity density has more severe impacts on soils, agriculture, droughts, and hazards in summer than in winter due the high impact of intense rainfalls.

In contrast to previous studies for Switzerland which were either limited spatially (to a few stations or a country) or temporally (to annual or seasonal R-factors) we were able to produce 12 monthly spatio-temporal maps. The maps are based on high resolution covariates in combination with an extended database of 87 automated gauging-stations recording in 10 min intervals, showing simultaneously spatial and temporal variations of R-factors. Regression-Kriging based on high spatio-temporal resolved covariates was successfully for most of the months (mean R^2=0.51, E_{RMS}=0.61 MJ mm ha^{-1} h^{-1} $month^{-1}$). It was used to map the long-term monthly mean R-factors based on an extended database of rain-gauging stations. The spatio-temporal mapping of rainfall erosivity and erosivity density revealed that intense rainfall events in August trigger the highest national mean value (263.5 MJ mm ha^{-1} h^{-1} $month^{-1}$). Especially the regions of Jura, Swiss Midland, northern Alpine foothill, and Ticino on the Southern Alps show pronounced rainfall erosivity during that month. The months June to September have a total share of 62% of the total annual rainfall erosivity in Switzerland.

The current data highlight that rainfall erosivity has a very high variability within a year. These trends of seasonality vary between regions and consequently support that a dynamic soil erosion and natural hazard risk assessment is crucial. The combination of the dynamic RUSLE-factors (R- and C-factor) will lead to a more realistic and time-dependent estimation of soil erosion within a year which is valuable for the identification of more susceptible seasons and regions as well as for the application of selective erosion control measures. A mapping of the seasonality of the C-factor for a subsequent synthesis to a dynamic soil erosion risk assessment for Switzerland is envisaged in a later study.

The findings of this study have a number of important implications for soil conservation planning. Based on the knowledge of the variability of rainfall erosivity, agronomists can introduce selective erosion control measures, a change in crop or crop rotation to weaken of the rainfalls impact on soils and vegetation by increasing soil cover or stabilizing topsoil during these susceptible months. As such, a targeted erosion control for Switzerland does not only reduce the direct costs of erosion by mitigation but also shrinks the costs for the implementation of control measures to a requested minimum.

Author contribution

S. Schmidt, K. Meusburger and C. Alewell analysed the data; S. Schmidt, K. Meusburger, C. Alewell, and P. Panagos wrote the paper.

Acknowledgement

The research has been funded by the Swiss Federal Office for the Environment (FOEN) (project N° N222-0350). We would like to thank MeteoSwiss, SwissTopo, and the cantons Lucerne, Berne, and St. Gallen for providing the datasets.

Conflict of interest

The authors confirm and sign that there is no conflict of interest with networks, organizations and data centers referred to in the paper.

References

Alewell, C., Meusburger, K., Juretzko, G., Mabit, L., and Ketterer, M. E.: Suitability of 239+240Pu and 137Cs as tracers for soil erosion assessment in mountain grasslands, Chemosphere, 103, 274–280, doi:10.1016/j.chemosphere.2013.12.016, 2014.

Arnhold, S., Lindner, S., Lee, B., Martin, E., Kettering, J., Nguyen, T. T., Koellner, T., Ok, Y. S., and Huwe, B.: Conventional and organic farming: Soil erosion and conservation potential for row crop cultivation, Geoderma, 219-220, 89–105, doi:10.1016/j.geoderma.2013.12.023, 2014.

Auerswald, K., Fiener, P., Gomez, J. A., Govers, G., Quinton, J. N., and Strauss, P.: Comment on "Rainfall erosivity in Europe" by Panagos et al. (Sci. Total Environ., 511, 801-814, 2015), The Science of the total environment, 532, 849–852, doi:10.1016/j.scitotenv.2015.05.019, 2015.

Avila Rangel, H. F. and Avila Rangel, B. D.: Spatial and temporal estimation of the erosivity factor R based on daily rainfall data for the department of Atlántico, Colombia, ing.inv., 35, 23–29, doi:10.15446/ing.investig.v35n2.47773, 2015.

Begert, M., Schlegel, T., and Kirchhofer, W.: Homogeneous temperature and precipitation series of Switzerland from 1864 to 2000, International Journal of Climatology, 25, 65–80, doi:10.1002/joc.1118, 2005.

Boardman, J. and Poesen, J. (Eds.): Soil erosion in Europe, Wiley-Interscience, Hoboken, NJ, 855 pp., 2006.

Bonilla, C. and Vidal, K.: Rainfall erosivity in Central Chile, Journal of Hydrology, 410, 126–133, doi:10.1016/j.jhydrol.2011.09.022, 2011.

Borrelli, P., Diodato, N., and Panagos, P.: Rainfall erosivity in Italy: A national scale spatio-temporal assessment, International Journal of Digital Earth, 1–16, doi:10.1080/17538947.2016.1148203, 2016.

Brown, L. and Foster, G.: Storm Erosivity Using Idealized Intensity Distributions, Transactions of the ASAE, 30, 379–386, doi:10.13031/2013.31957, 1987.

da Silva, A. M., Wiecheteck, M., and Zuercher, B. W.: Spatial Assessment of Indices for Characterizing the Erosive Force of Rainfall in El Salvador Republic, Environmental Engineering Science, 28, 309–316, doi:10.1089/ees.2010.0296, 2011.

Dabney, S. M., Yoder, D. C., Vieira, D., and Bingner, R. L.: Enhancing RUSLE to include runoff-driven phenomena, Hydrol. Process., 25, 1373–1390, doi:10.1002/hyp.7897, 2011.

Dabney, S. M., Yoder, D. C., and Vieira, D. A. N.: The application of the Revised Universal Soil Loss Equation, Version 2, to evaluate the impacts of alternative climate change scenarios on runoff and sediment yield, Journal of Soil and Water Conservation, 67, 343–353, doi:10.2489/jswc.67.5.343, 2012.

Efron, B. and Tibshirani, R.: Improvements on Cross-Validation: The .632+ Bootstrap Method, Journal of the American Statistical Association, 92, 548, doi:10.2307/2965703, 1997.

Foster, G. R., Yoder, D. C., Weesies, G. A., McCool, D. K., McGregor, K. C., and Bingner, R.: Draft User's Guide, Revised Universal Soil Loss Equation Version 2 (RUSLE-2), Washington, DC, 2008.

Friedli, S.: Digitale Bodenerosionsgefährdungskarte Der Schweiz Im Hektarraster – Unter Besonderer Berücksichtigung des Ackerlandes, Bern, 2006.

Fuhrer, J., Beniston, M., Fischlin, A., Frei, C., Goyette, S., Jasper, K., and Pfister, C.: Climate Risks and Their Impact on Agriculture and Forests in Switzerland, Climatic Change, 79, 79–102, doi:10.1007/s10584-006-9106-6, 2006.

Gisler, S., Lininger, H.-P., and Prasuhn, V.: Erosionsrisikokarte im 2x2-Meter-Raster (ERK2), Agrarforschung Schweiz, 2, 2011.

Harrell Jr., F.: Regression Modeling Strategies: With Applications to Linear Models, Logistic and Ordinal Regression, and Survival Analysis, Cham, 2015.

Hartwig, N. L. and Ammon, H. U.: Cover crops and living mulches, Weed Science, 50, 688–699, doi:10.1614/0043-1745(2002)050[0688:AIACCA]2.0.CO;2, 2002.

Hengl, T., Heuvelink, G., and Rossiter, D.: About regression-kriging: From equations to case studies, Computers & Geosciences, 33, 1301–1315, doi:10.1016/j.cageo.2007.05.001, 2007.

Hengl, T., Heuvelink, G., and Stein, A.: A generic framework for spatial prediction of soil variables based on regression-kriging, Geoderma, 120, 75–93, doi:10.1016/j.geoderma.2003.08.018, 2004.

Hengl, T.: A practical guide to geostatistical mapping of environmental variables, EUR, 22904EN, Publications Office, Luxembourg, 2007.

Hurni, H.: Bestimmung der Erosivität von Hagelereignissen: Empirische Bestimmung der Erosivität von Hagelereignissen, Unpublished manuscript, 1978.

Isotta, F., Frei, C., Weilguni, V., Perčec T., M., Lassègues, P., Rudolf, B., Pavan, V., Cacciamani, C., Antolini, G., Ratto, S., Munari, M., Micheletti, S., Bonati, V., Lussana, C., Ronchi, C., Panettieri, E., Marigo, G., and Vertačnik, G.: The climate of daily precipitation in the Alps: Development and analysis of a high-resolution grid dataset from pan-Alpine rain-gauge data, International Journal of Climatology), 34, 1657–1675, doi:10.1002/joc.3794, 2014.

Jensen, H., Lang, H., and Rinderknecht, J.: Extreme Point Rainfall of Varying Duration and Return Period 1901-1970, in: Hydrological Atlas of Switzerland, Wingartner, R. (Ed.), Bern, 2007.

Konz, N., Prasuhn, V., and Alewell, C.: On the measurement of alpine soil erosion, CATENA, 91, 63–71, doi:10.1016/j.catena.2011.09.010, 2012.

Köppen, W.: Das geographische System der Klimate, Handbuch der Klimatologie, 1, Berlin, 1936.

Kulikov, M., Schickhoff, U., and Borchardt, P.: Spatial and seasonal dynamics of soil loss ratio in mountain rangelands of south-western Kyrgyzstan, J. Mt. Sci., 13, 316–329, doi:10.1007/s11629-014-3393-6, 2016.

Lai, C., Xiaohong, C., Zhaoli, W., Xushu, W., Shiwei, Z., Xiaoqing, W., and Wenkui, B.: Spatio-temporal variation in rainfall erosivity during 1960–2012 in the Pearl River Basin, China, CATENA, 137, 382–391, doi:10.1016/j.catena.2015.10.008, 2016.

Ledermann, T.: Multiple Implications of Soil Erosion and Conservation on Arable Farm Land in the Swiss Midlands, Bern, 2012.

Leek, R. and Olsen, P.: Modelling climatic erosivity as a factor for soil erosion in Denmark: Changes and temporal trends, Soil Use and Management, 16, 61–65, doi:10.1111/j.1475-2743.2000.tb00175.x, 2000.

Ma, X., He, Y., Xu, J., van Noordwijk, M., and Lu, X.: Spatial and temporal variation in rainfall erosivity in a Himalayan watershed, CATENA, 121, 248–259, doi:10.1016/j.catena.2014.05.017, 2014.

Marxer, P.: Oberflächenabfluß und Bodenerosion auf Brandflächen des Kastanienwaldgürtels der Südschweiz mit einer Anleitung zur Bewertung der post-fire Erosionsanfälligkeit (BA EroKaBr), Physiogeographica, 33, Wepf in Komm, Basel, 2003.

Meshesha, D., Tsunekawa, A., Tsubo, M., Haregeweyn, N., and Adgo, E.: Evaluating spatial and temporal variations of rainfall erosivity, case of Central Rift Valley of Ethiopia, Theor Appl Climatol, 119, 515–522, doi:10.1007/s00704-014-1130-2, 2015.

MeteoSchweiz: Klimaszenarien Schweiz: eine regionale Übersicht, Bern, 2013.

MeteoSwiss: Documentation of MeteoSwiss Grid-Data Products: Monthly and Yearly Preciüitation: RhiresM and RhiresY, Zürich, 2013.

Meusburger, K. and Alewell, C.: Impacts of anthropogenic and environmental factors on the occurrence of shallow landslides in an alpine catchment (Urseren Valley, Switzerland), Nat. Hazards Earth Syst. Sci., 8, 509–520, doi:10.5194/nhess-8-509-2008, 2008.

Meusburger, K., Steel, A., Panagos, P., Montanarella, L., and Alewell, C.: Spatial and temporal variability of rainfall erosivity factor for Switzerland, Hydrol. Earth Syst. Sci., 16, 167–177, doi:10.5194/hess-16-167-2012, 2012.

Mosimann, T., Crole-Rees, A., Maillard, A., Neyroud, J.-A., Thöni, M., Musy, A., and Rohr, W.: Bodenerosion im Schweizerischen Mittelland: Ausmass und Gegenmassnahmen, Bericht 51 des Nationalen Forschungsprogrammes Nutzung des Bodens in der Schweiz, Liebefeld-Bern, 1990.

Mosimann, T., Maillard, A., Musy, A., Neyroud, J.-A., Rüttimann, M., and Weisskopf, P.: Erosionsbekämpfung in Ackerbaugebieten: Ein Leitfaden für die Bodenerhaltung, Themenbericht des NAtionalen Forschungsprogrammes "Nutzung des Bodes in der Schweiz", 1991.

Nogler, S.: Erosvität der Niederschläge im schweizerischen Mittelland, Bern, 2012.

Panagos, P., Ballabio, C., Borrelli, P., and Meusburger, K.: Spatio-temporal analysis of rainfall erosivity and erosivity density in Greece, CATENA, 137, 161–172, doi:10.1016/j.catena.2015.09.015, 2016b.

Panagos, P., Ballabio, C., Borrelli, P., Meusburger, K., Klik, A., Rousseva, S., Tadić, M., Michaelides, S., Hrabalíková, M., Olsen, P., Aalto, J., Lakatos, M., Rymszewicz, A., Dumitrescu, A., Beguería, S., and Alewell, C.: Rainfall erosivity in Europe, The Science of the total environment, 511, 801–814, doi:10.1016/j.scitotenv.2015.01.008, 2015a.

Panagos, P., Borrelli, P., Spinoni, J., Ballabio, C., Meusburger, K., Beguería, S., Klik, A., Michaelides, S., Petan, S., Hrabalíková, M., Olsen, P., Aalto, J., Lakatos, M., Rymszewicz, A., Dumitrescu, A., Perčec Tadić, M., Diodato, N., Kostalova, J., Rousseva, S., Banasik, K., and Alewell, C.: Monthly Rainfall Erosivity: Conversion Factors for Different Time Resolutions and Regional Assessments, Water, 8, 119, doi:10.3390/w8040119, 2016b.

Panagos, P., Meusburger, K., Ballabio, C., Borrelli, P., Beguería, S., Klik, A., Rymszewicz, A., Michaelides, S., Olsen, P., Tadić, M. P., Aalto, J., Lakatos, M., Dumitrescu, A., Rousseva, S., Montanarella, L., and Alewell, C.: Reply to the comment on "Rainfall erosivity in Europe" by Auerswald et al, The Science of the total environment, 532, 853–857, doi:10.1016/j.scitotenv.2015.05.020, 2015b.

Perroud, M. and Bader, S.: Klimaänderung in der Schweiz. Indikatoren zu Ursachen, Auswirkungen, Massnahmen., Umwelt-Zustand, 2013.

Prasuhn, V.: Soil erosion in the Swiss midlands: Results of a 10-year field survey, Geomorphology, 126, 32–41, doi:10.1016/j.geomorph.2010.10.023, 2011.

Prasuhn, V.: On-farm effects of tillage and crops on soil erosion measured over 10 years in Switzerland, Soil and Tillage Research, 120, 137–146, doi:10.1016/j.still.2012.01.002, 2012.

Prasuhn, V., Liniger, H., Gisler, S., Herweg, K., Candinas, A., and Clément, J.-P.: A high-resolution soil erosion risk map of Switzerland as strategic policy support system, Land Use Policy, 32, 281–291, doi:10.1016/j.landusepol.2012.11.006, 2013.

Renard, K., Foster, G., Weesies, G., and Porter, J.: RUSLE: Revised universal soill loss equation, Journal of Soil and Water Conservation, 46, 1991.

Renard, K. G., Foster, G., Weesies, G., McCool, D. K., and Yoder, D. C.: Prediction Soil Erosion by Water: A Guide to Conservation Planning with the Revised Universal Soil Loss Equation (RUSLE), Agriculture handbook, 703, 1997.

Sadeghi, S., Moatamednia, M., and Behzadfar, M.: Spatial and Temporal Variations in the Rainfall Erosivity Factor in Iran, J. Agr. Sci. Tech., 451–464, 2011.

Schwarb, M., Daly, C., Frei, C., and Schär, C.: Mean Seasonal Precipitation throughout the European Alps 1971-1990, in: Hydrological Atlas of Switzerland, Wingartner, R. (Ed.), Bern, 2007.

Schwertmann, U., Vogl, W., and Kainz, M.: Bodenerosion durch Wasser: Vorhersage des Abtrags und Bewertung von Gegenmaßnahmen, Stuttgart, 64 pp., 1987.

Sideris, I., Gabella, M., and Germann, U.: The CombiPrecip experience: development and operation of a real-time radar-raingauge combination scheme in Switzerland, 2014 International Weather Radar and Hydrology Symposium (Ed.), 2014.

Spreafico, M. and Weingartner, R.: Hydrologie der Schweiz: Ausgewählte Aspekte und Resultate, Berichte des BWG, Serie Wasser, 2005.

Steyerberg, E.: Clinical Prediction Models: A Practical Approach to Development, Validation, and Updating, New York, NY, 2009.

Torriani, D. S., Calanca, P., Schmid, S., Beniston, M., and Fuhrer, J.: Potential effects of changes in mean climate and climate variability on the yield of winter and spring crops in Switzerland, Clim. Res., 34, 59–69, doi:10.3354/cr034059, 2007.

Wang, G., Gertner, G., Singh, V., Shinkareva, S., Parysow, P., and Anderson, A.: Spatial and temporal prediction and uncertainty of soil loss using the revised universal soil loss equation: A case study of the rainfall–runoff erosivity R factor, Ecological Modelling, 153, 143–155, doi:10.1016/S0304-3800(01)00507-5, 2002.

Weisshaidinger, R. and Leser, H.: Switzerland, in: Soil erosion in Europe, Boardman, J., Poesen, J. (Eds.), Wiley-Interscience, Hoboken, NJ, 2006.

Wellinger, R., Buser, H.-P., Krauss, J., and Theiler, R.: Karotten: Anbau, Erntezeitpunkt und Lagerung, Agrarforschung Schweiz, 13, 412–417, 2006.

Wingartner, R. (Ed.): Hydrological Atlas of Switzerland, Bern, 2007.

Wischmeier, W. H. and Smith, D. D.: Predicting rainfall erosion losses, Agriculture handbook, 537, U.S. Gov. Print. Off, Washington, 58 pp., 1978.

Yang, X. and Yu, B.: Modelling and mapping rainfall erosivity in New South Wales, Australia, Soil Res., doi:10.1071/SR14188, 2015.

Zhao, Q., Liu, Q., Ma, L., Ding, S., Xu, S., W., C., and Liu, P.: Spatiotemporal variations in rainfall erosivity during the period of 1960–2011 in Guangdong Province, southern China, Theor Appl Climatol, doi:10.1007/s00704-015-1694-5, 2015.

Hydrol. Earth Syst. Sci. Discuss., doi:10.5194/hess-2016-208, 2016
Manuscript under review for journal Hydrol. Earth Syst. Sci.
Published: 9 May 2016

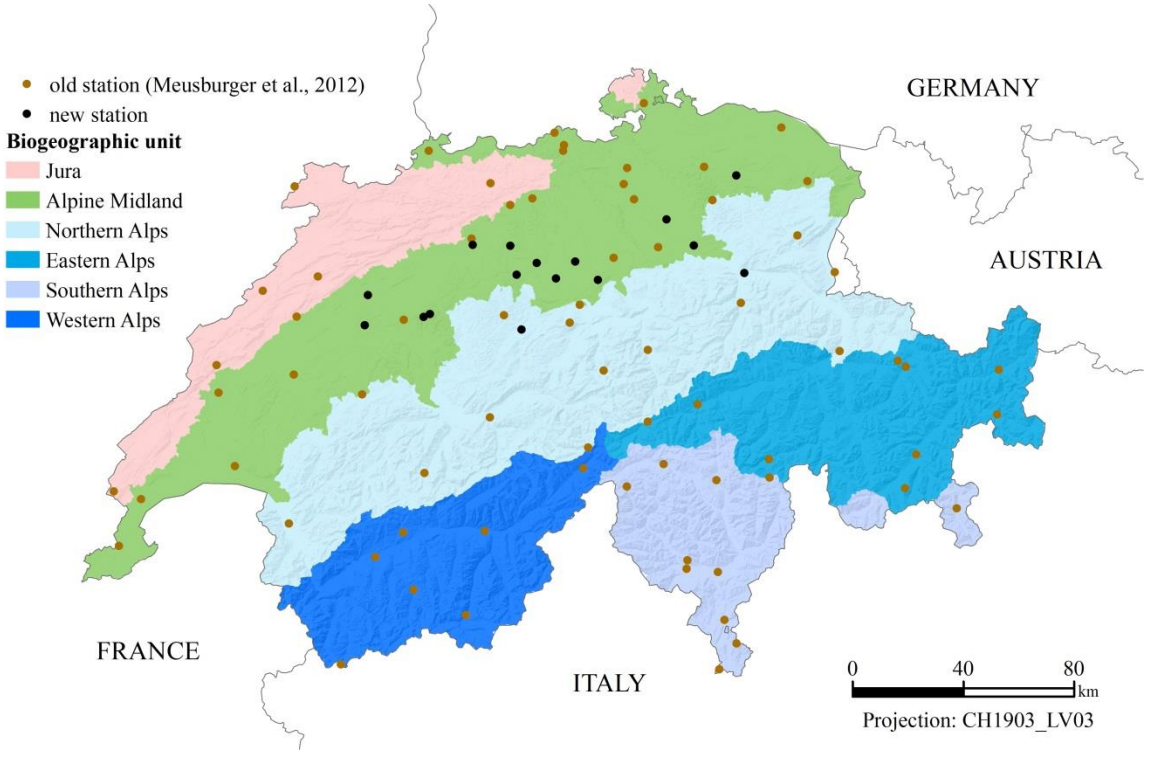

Figure 1: Biogeographic units and used gauging stations in Switzerland.

Hydrol. Earth Syst. Sci. Discuss., doi:10.5194/hess-2016-208, 2016
Manuscript under review for journal Hydrol. Earth Syst. Sci.
Published: 9 May 2016

Hydrology and Earth System Sciences
Open Access
Discussions

Table 1: Datasets used as covariates for the spatio-temporal mapping of rainfall erosivity.

dataset	derived information	temporal resolution	spatial resolution	measuring period	source
Total snow depth	long-term monthly snow depth	hourly	58 stations	1988 – 2010	MeteoSwiss
CombiPrecip	long-term monthly mean rainfall amount from measured and radar data	hourly	1 km	2005 – 2015	Sideris et al., 2014
EURO4M-APGD	long-term mean daily precipitation per month	monthly	5 km	1971 – 2008	Isotta et al., 2014
RhiresM	long-term mean monthly precipitation sums	monthly	1 km	1961 – 2015	MeteoSwiss, 2013
SwissAlti3D	elevation, slope, aspect	-	2 m	-	SwissTopo

Hydrol. Earth Syst. Sci. Discuss., doi:10.5194/hess-2016-208, 2016
Manuscript under review for journal Hydrol. Earth Syst. Sci.
Published: 9 May 2016

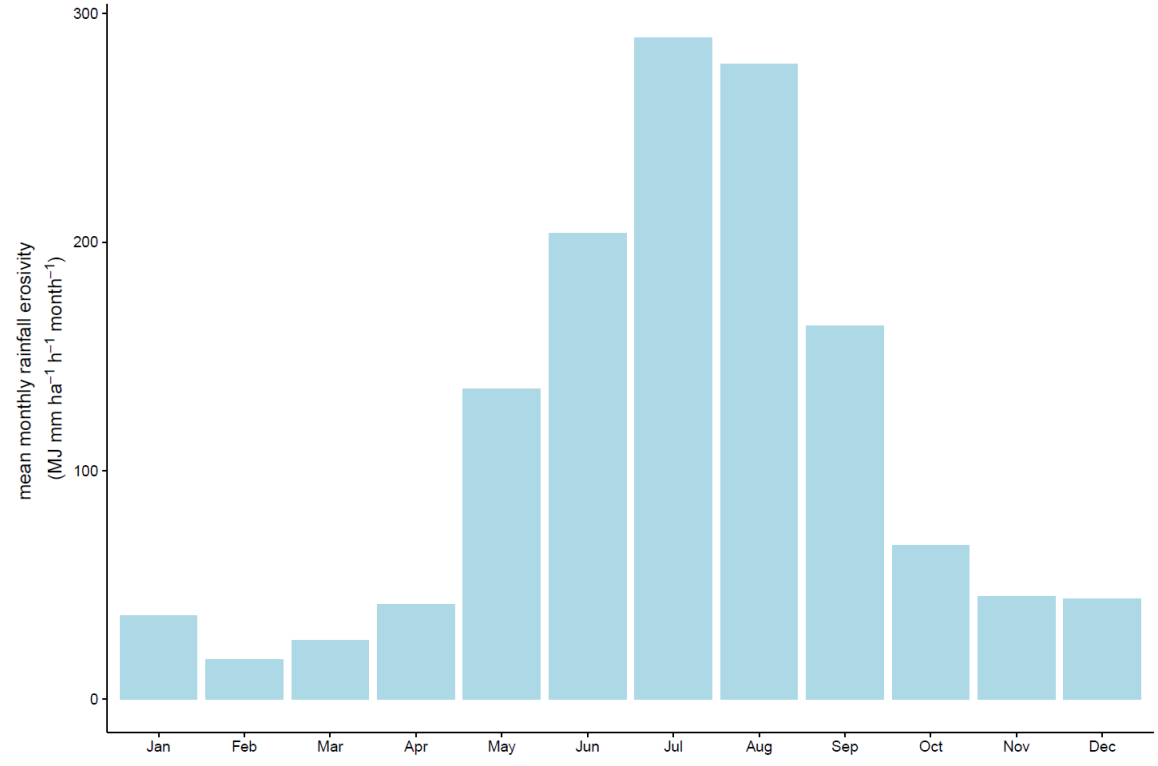

Figure 2: Mean monthly rainfall erosivity for all 87 Swiss stations.

Hydrol. Earth Syst. Sci. Discuss., doi:10.5194/hess-2016-208, 2016
Manuscript under review for journal Hydrol. Earth Syst. Sci.
Published: 9 May 2016

Hydrology and Earth System Sciences
Open Access
Discussions

Table 2: Regression equations and selected covariates for estimating mean monthly rainfall erosivity in Switzerland.

Month	Regression equation
January	$R_{Jan} = 2.101 - 4.150 \cdot CombiPrecip_{Jan} - 0.006 \cdot Snow\ depth_{Jan} + 0.017 \cdot Rhires_{Jan} - 0.001 \cdot Elevation$
February	$R_{Feb} = 2.702 - 13.812 \cdot CombiPrecip_{Feb} - 0.007 \cdot Snow\ depth_{Feb} + 0.019 \cdot Rhires_{Feb} + 0.211 \cdot Alpine\ Precip_{Feb} - 0.001 \cdot Elevation$
March	$R_{Mar} = 2.534 - 7.735 \cdot CombiPrecip_{Mar} - 0.006 \cdot Snow\ depth_{Mar} + 0.018 \cdot Rhires_{Mar} + 0.170 \cdot Alpine\ Precip_{Mar} - 0.001 \cdot Elevation$
April	$R_{Apr} = 2.330 - 3.319 \cdot CombiPrecip_{Apr} - 0.008 \cdot Snow\ depth_{Apr} + 0.023 \cdot Rhires_{Apr} - 0.001 \cdot Elevation - 0.019 \cdot Slope$
May	$R_{May} = 2.965 + 2.072 \cdot CombiPrecip_{May} - 0.002 \cdot Snow\ depth_{May} + 0.015 \cdot Rhires_{May} - 0.001 \cdot Elevation$
June	$R_{Jun} = 3.890 + 0.014 \cdot Rhires_{Jun} - 0.001 \cdot Elevation$
July	$R_{Jul} = 3.926 + 5.710 \cdot CombiPrecip_{Jul} + 0.251 \cdot Alpine\ Precip_{Jul} - 0.001 \cdot Elevation$
August	$R_{Aug} = 3.627 + 0.010 \cdot Rhires_{Aug} + 0.194 \cdot Alpine\ Precip_{Aug} - 0.001 \cdot Elevation$
September	$R_{Sep} = 2.760 + 2.243 \cdot CombiPrecip_{Sep} + 0.539 \cdot Alpine\ Precip_{Sepb} - 0.001 \cdot Elevation$
October	$R_{Oct} = 2.753 + 0.0161 \cdot Rhires_{Oct} - 0.001 \cdot Elevation$
November	$R_{Nov} = 2.665 + 3.787 \cdot CombiPrecip_{Nov} - 0.034 \cdot Snow\ depth_{Nov} + 0.166 \cdot Alpine\ Precip_{Nov}$
December	$R_{Dec} = 2.437 + 0.013 \cdot Rhires_{Dec} - 0.001 \cdot Elevation$

Hydrol. Earth Syst. Sci. Discuss., doi:10.5194/hess-2016-208, 2016
Manuscript under review for journal Hydrol. Earth Syst. Sci.
Published: 9 May 2016

Hydrology and Earth System Sciences
Discussions

Table 3: Model efficiency by R^2 and E_{RMS} and omitted outliers and influential observations per month.

Month	Excl. outlier stations	R^2	E_{RMS}	Null Deviance	Res. deviance
January	Mathod	0.52	0.66	70.36	20.65
February	Monte Generoso, Napf, Saetis	0.53	0.72	79.28	31.82
March	Col du Grand St-Bernard, Saetis	0.49	0.63	61.45	21.84
April	Col du Grand St-Bernard, Saetis, Weissfluhjoch	0.65	0.52	63.69	15.90
May	Davos, Col du Grand St-Bernard	0.60	0.53	56.28	16.83
June	Col du Grand St-Bernard	0.58	0.54	51.61	19.31
July	Monte Generoso, Col du Grand St-Bernard, Stabio	0.66	0.42	38.58	11.57
August	Col du Grand St-Bernard, Stabio	0.47	0.61	50.47	21.75
September	Col du Grand St-Bernard, Stabio	0.64	0.54	61.23	16.27
October	Piz Corvatsch, Col du Grand St-Bernard, Stabio	0.62	0.42	37.86	12.07
November	Piz Corvatsch, Col du Grand St-Bernard, Saetis	0.10	0.93	58.85	47.22
December	Col du Grand St-Bernard	0.26	0.85	73.90	50.66

Hydrol. Earth Syst. Sci. Discuss., doi:10.5194/hess-2016-208, 2016
Manuscript under review for journal Hydrol. Earth Syst. Sci.
Published: 9 May 2016

Table 4: Monthly national rainfall erosivity in MJ mm ha^{-1} h^{-1} ~~month~~$^{-1}$.

Month	Minima	Maxima	Mean
January	0.2	71.3	10.5
February	0.0	247.3	13.5
March	0.0	179.0	20.1
April	0.2	1014.4	28.8
May	8.3	1717.8	120.2
June	3.6	1262.1	174.8
July	12.6	1481.1	255.4
August	8.3	1994.9	263.5
September	6.8	6107.9	147.7
October	5.7	977.0	57.0
November	4.9	357.1	41.6
December	1.3	234.4	24.9

Hydrol. Earth Syst. Sci. Discuss., doi:10.5194/hess-2016-208, 2016
Manuscript under review for journal Hydrol. Earth Syst. Sci.
Published: 9 May 2016

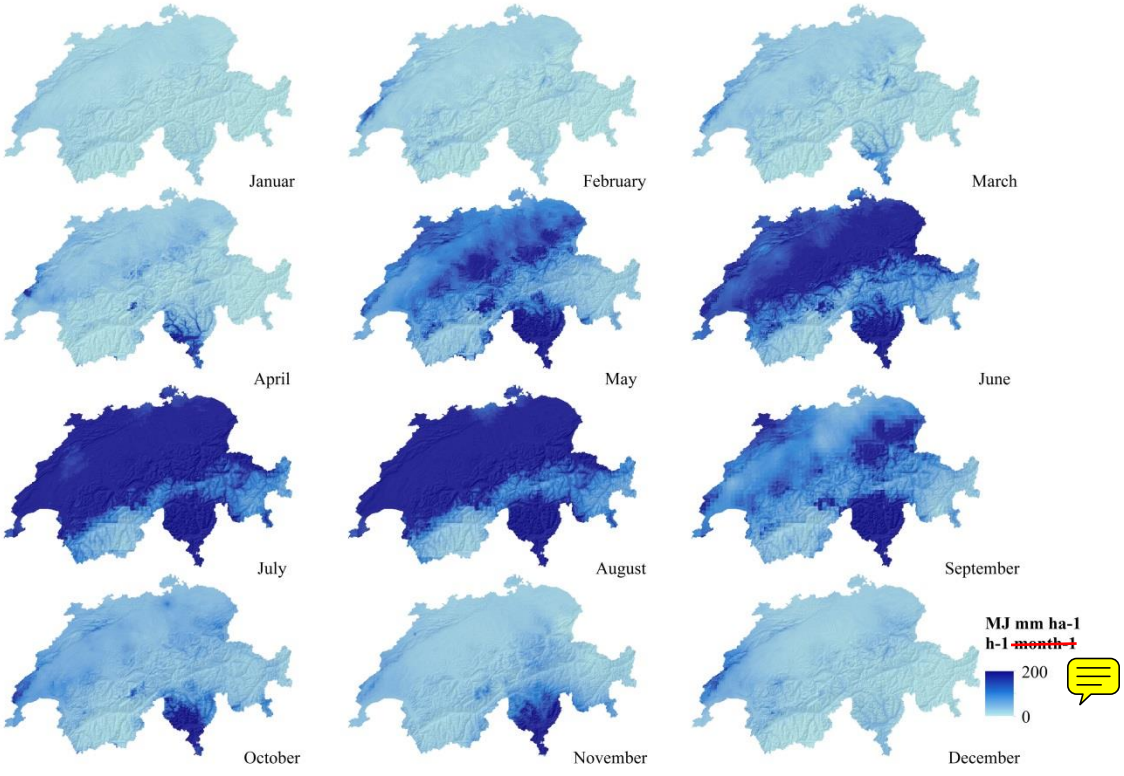

Figure 3: Monthly rainfall erosivity maps for Switzerland (equal stretch from 0 to 200 MJ mm ha^{-1} h^{-1} ~~month^{-1}~~) derived by regression-kriging.

Hydrol. Earth Syst. Sci. Discuss., doi:10.5194/hess-2016-208, 2016
Manuscript under review for journal Hydrol. Earth Syst. Sci.
Published: 9 May 2016

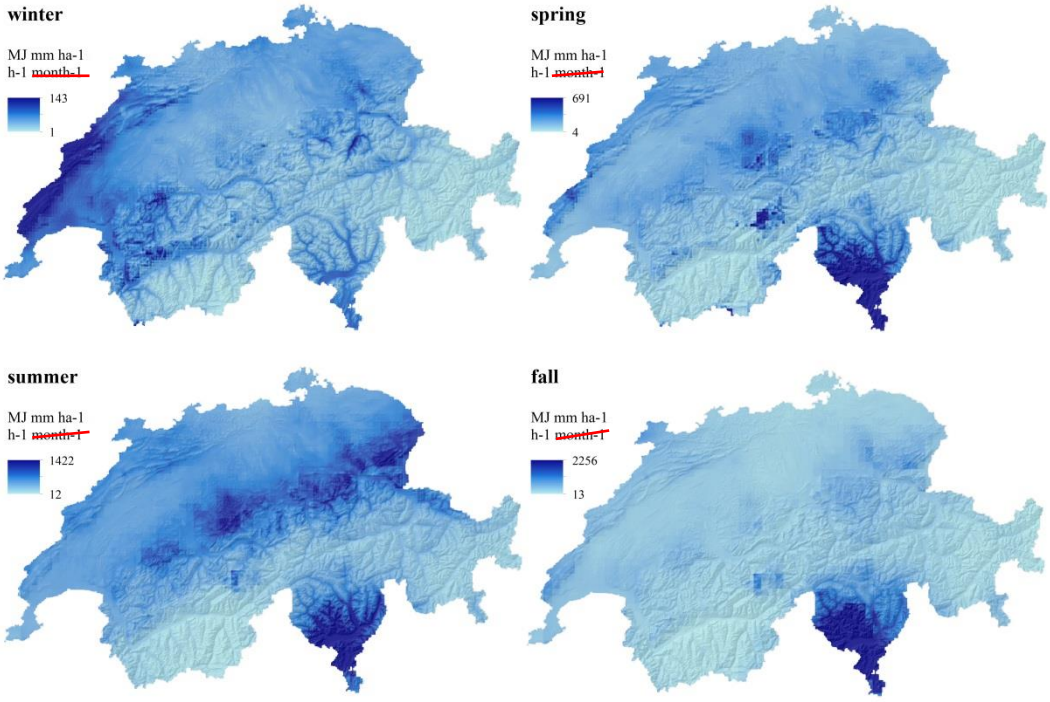

Figure 4: Seasonal rainfall erosivity maps for Switzerland derived by regression-kriging. The following months were averaged to derive seasonal maps: winter (Dec-Feb), spring (Mar-May), summer (Jun-Sep), fall (Oct-Nov).

Hydrol. Earth Syst. Sci. Discuss., doi:10.5194/hess-2016-208, 2016
Manuscript under review for journal Hydrol. Earth Syst. Sci.
Published: 9 May 2016

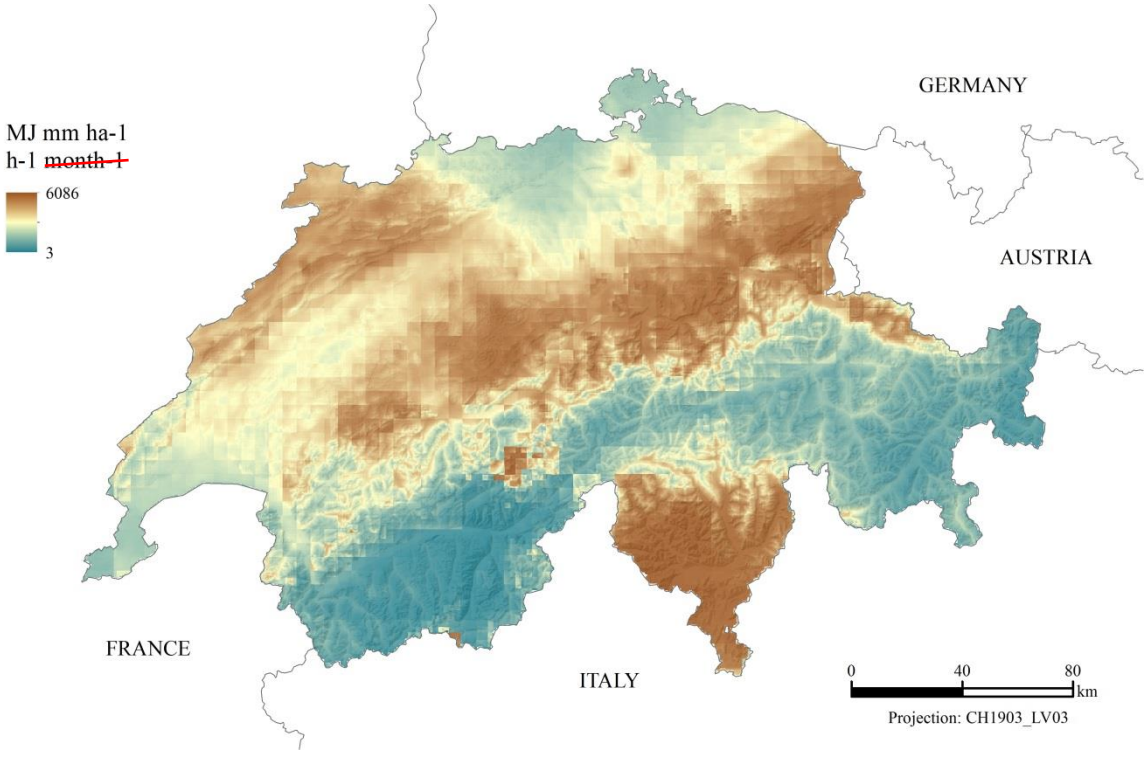

Figure 5: Range map for Switzerland showing the variability of ~~monthly~~ rainfall erosivity among a year.

Hydrol. Earth Syst. Sci. Discuss., doi:10.5194/hess-2016-208, 2016
Manuscript under review for journal Hydrol. Earth Syst. Sci.
Published: 9 May 2016

Hydrology and Earth System Sciences
Discussions

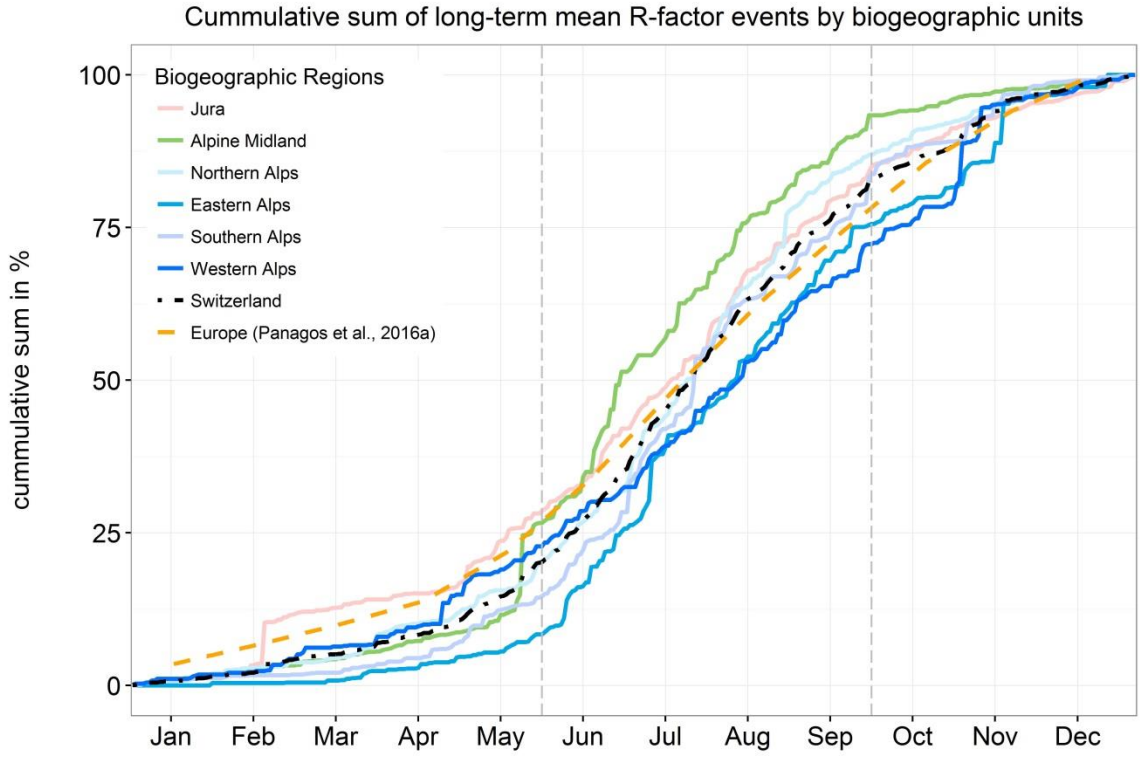

Figure 6: Cumulative daily rainfall erosivity proportion for Swiss biogeographic units, Switzerland and monthly rainfall erosivity for Europe (linear smoothed, European data from Panagos et al., 2016a).

Hydrol. Earth Syst. Sci. Discuss., doi:10.5194/hess-2016-208, 2016
Manuscript under review for journal Hydrol. Earth Syst. Sci.
Published: 9 May 2016

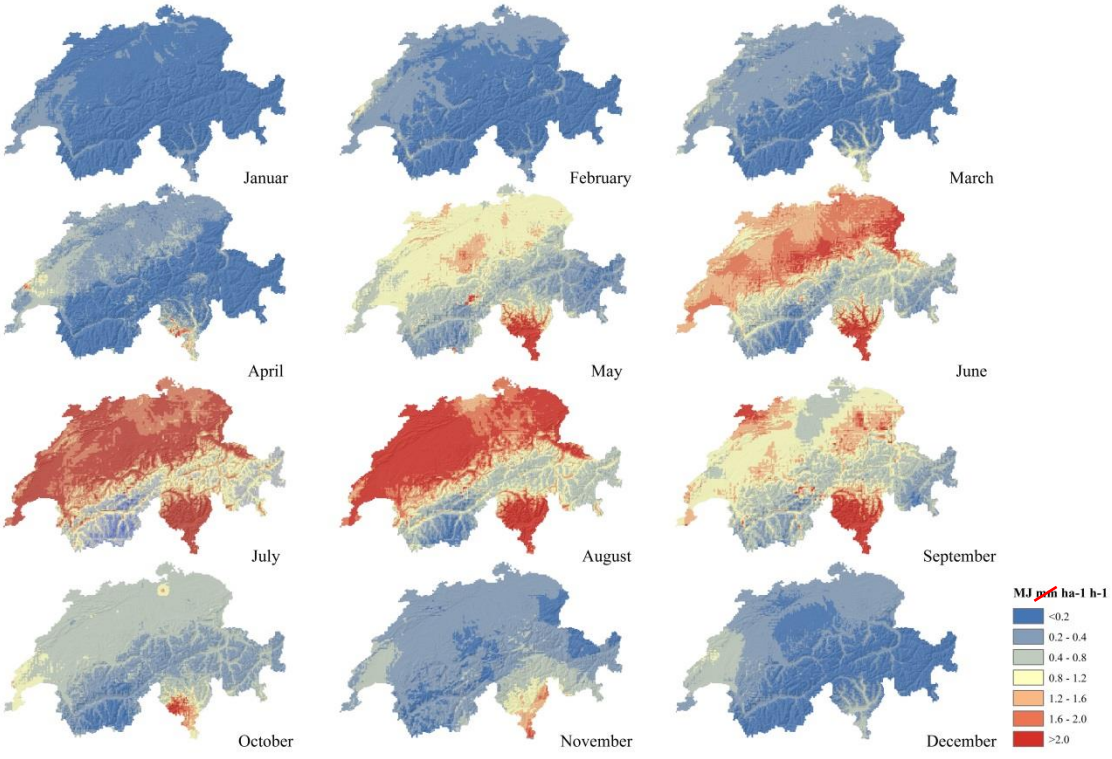

Figure 7: Monthly erosivity density for Switzerland as ratio of monthly rainfall erosivity to monthly precipitation amount.

Hydrol. Earth Syst. Sci. Discuss., doi:10.5194/hess-2016-208, 2016
Manuscript under review for journal Hydrol. Earth Syst. Sci.
Published: 9 May 2016

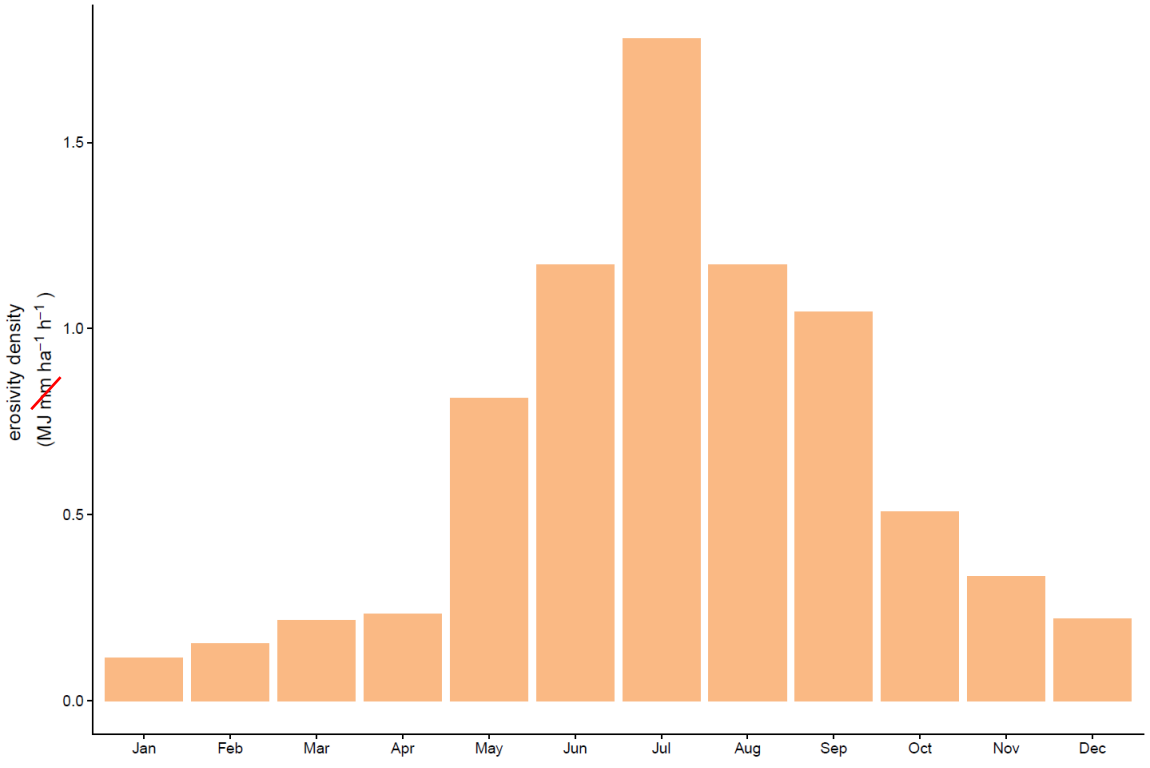

Figure 8: Monthly erosivity density for Switzerland.